

Intraoperative ultrasonography for the correction of brainshift based on the matching of hyperechogenic structures

Pierrick Coupé, Pierre Hellier, Xavier Morandi, Christian Barillot

► **To cite this version:**

Pierrick Coupé, Pierre Hellier, Xavier Morandi, Christian Barillot. Intraoperative ultrasonography for the correction of brainshift based on the matching of hyperechogenic structures. IEEE International Symposium on Biomedical Imaging, Apr 2010, Rotterdam, Netherlands. pp.1405 - 1408, 10.1109/ISBI.2010.5490261 . inserm-00515405

HAL Id: inserm-00515405

<https://www.hal.inserm.fr/inserm-00515405>

Submitted on 8 Sep 2010

HAL is a multi-disciplinary open access archive for the deposit and dissemination of scientific research documents, whether they are published or not. The documents may come from teaching and research institutions in France or abroad, or from public or private research centers.

L'archive ouverte pluridisciplinaire **HAL**, est destinée au dépôt et à la diffusion de documents scientifiques de niveau recherche, publiés ou non, émanant des établissements d'enseignement et de recherche français ou étrangers, des laboratoires publics ou privés.

INTRAOPERATIVE ULTRASONOGRAPHY FOR THE CORRECTION OF BRAINSHIFT BASED ON THE MATCHING OF HYPERECHOGENIC STRUCTURES

Pierrick Coupé^{1,2,3}, Pierre Hellier^{1,2,3}, Xavier Morandi^{1,2,3,4} and Christian Barillot^{1,2,3}

¹ University of Rennes I, UMR CNRS 6074, IRISA, Rennes, France, ² INRIA, VisAGeS U746 Unit/Project, Rennes, France

³ INSERM, VisAGeS U746 Unit/Project, Rennes, France, ⁴ CHU, University Hospital of Rennes, Rennes, France

ABSTRACT

In this paper, a global approach based on 3D freehand ultrasound imaging is proposed to (a) correct the error of the neuronavigation system in image-patient registration and (b) compensate for the deformations of the cerebral structures occurring during a neurosurgical procedure. The rigid and non rigid multimodal registrations are achieved by matching the hyperechogenic structures of brain. The quantitative evaluation of the non rigid registration was performed within a framework based on synthetic deformation. Finally, experiments were carried out on real data sets of 4 patients with lesions such as cavernoma and low-grade glioma. Qualitative and quantitative results on the estimated error performed by neuronavigation system and the estimated brain deformations are given.

Index Terms— multimodal registration, non rigid deformation, neurosurgery, brainshift, freehand ultrasound

1. INTRODUCTION

In Image-Guided NeuroSurgery (IGNS), the accuracy and usefulness of the neuronavigation system is limited due to the presence of soft-tissue deformations. This phenomenon also known as brainshift is the motion of cerebral structures occurring after the craniotomy (up to 25 mm [1, 2, 3]). The neuronavigation system rigidly matches the pre-operative images with the surgical field. The hypothesis of a rigid registration is no longer valid because of deformations. In order to compensate for brainshift, many approaches have been investigated. In this paper, we focus on methods using intraoperative ultrasound imaging (iUS) to achieve image registration [3, 4, 5, 6, 7, 8]. These methods have studied three options to register US and MR images : the matching of homologous features extracted from both images [7, 6], the preprocessing of the images to make US images and MR images more similar in order to use classical similarity measures [5, 3], and the intensity-based registration based on a specific similarity measure matching the US and MR image intensities [4, 9]. In this paper, a global approach based on image registration of intraoperative freehand ultrasound imaging and preoperative MR image is proposed to (a) correct the error of the neuronavigation system in image-patient registration and (b) compen-

sate for the deformations of the cerebral structures occurring during a neurosurgical procedure. To do this, a multimodal registration of 3D iUS with preoperative MR images is rigidly performed before opening the dura and non-rigidly performed after opening the dura. As it is generally admitted, we assume that no significant brainshift occurs before opening of the dura. This paper proposes a general framework designed for brainshift compensation built on previous works on 3D reconstruction of freehand US [10], denoising of US images [11] and rigid registration of US and MR images [9].

2. METHOD

2.1. Similarity function

Contrary to histogram-based approaches [4, 3], the method proposed in [9] consists in matching the informative features present in US images which are the hyperechogenic structures. After computing probability maps, defined for a voxel $X = (x, y, z)$ as the probability to be included in hyperechogenic from the both modalities, the rigid transformation \hat{T} is estimated by maximizing the conjoint probability :

$$\hat{T} = \arg \max_T \int_{\Omega} p(X \in \Phi_{US}, T(X) \in \Phi_{MR}) dX \quad (1)$$

where $p(X \in \Phi_{US})$ is the probability for X to be included in an hyperechogenic structure of the US image and $p(X \in \Phi_{MR})$ is the probability for X to be included in an hyperechogenic structure (in the sense of the ultrasound image) of the MR image. Assuming observations are independent, this yields :

$$\hat{T} = \arg \max_T \int_{\Omega} p(X \in \Phi_{US}) \cdot p(T(X) \in \Phi_{MR}) dX \quad (2)$$

The construction of the probability maps from both modalities are based on different approaches. For intraoperative US images, a normalization of the intensities is performed during surgery to obtain $p(X \in \Phi_{US}) \in [0, 1]$. For preoperative MR image, the probability for a voxel X to be included in an hyperechogenic structure is based both on the $MLvv$ operator [12] (Ridge Seeking operator) and the manual segmentation of the pathological tissue performed by the neurosurgeon. The

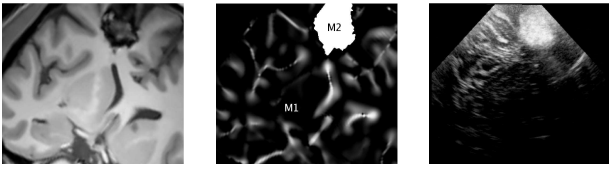


Fig. 1. Left : the denoised MR images. Middle : the probability map based on $MLvv$ and tumor segmentation. Right : the corresponding US images obtained with the registration provided by the neuronavigation system.

probability $p(X \in \Phi_{MR})$ is computed before surgery on a T1-weighted MR image as follows :

$$p(X \in \Phi_{MR}) = \begin{cases} MLvv(I(X)) & \text{if } X \in M_1 \\ \Psi(X) & \text{if } X \in M_2 \\ 0 & \text{otherwise} \end{cases} \quad (3)$$

where I is the intensity function, M_1 represents the positive values of $MLvv$ map (i.e. the sulci and the cerebral falx) normalized between $[0, 1]$ and computed on the brain tissue without the pathological tissue segmentation M_2 (see Fig. 1 and [9] for details). $\Psi(X)$ is the probability given to X in the segmentation of pathological tissue M_2 and $\Psi(\cdot)$ is used to incorporate *a priori* on pathology. For hyperechogenic pathological tissue such as cavernoma or low-grade glioma $\Psi(X)$ is high (close to 1).

2.2. Non rigid transformation

In this paper, the registration method is extended to non rigid transformations. The non rigid transformation is projected on cosine basis functions defined by their pulsation ω^f (i.e. frequency) [13]. During the procedure, the magnitude parameters ($\{\alpha_i^f, \beta_i^f, \gamma_i^f; i \in [1, 2, 3]\}$) and phases parameters ($\{\phi_i^f, \psi_i^f, \rho_i^f; i \in [1, 2, 3]\}$) are estimated for each cosine basis function. The set of pulsations \mathcal{W} of the basis functions is defined as $\mathcal{W} : \{\omega^1, \dots, \omega^F\}$ and is fixed *a priori*. This set has been empirically established thanks to the experiment on synthetic deformation. Finally, the parametrization can be written as :

$$\begin{aligned} u_1^F(x, y, z) &= \sum_{f=1}^F (\alpha_1^f \cos(\omega^f x + \phi_1^f) + \beta_1^f \cos(\omega^f y + \psi_1^f) + \gamma_1^f \cos(\omega^f z + \rho_1^f)) \\ u_2^F(x, y, z) &= \sum_{f=1}^F (\alpha_2^f \cos(\omega^f x + \phi_2^f) + \beta_2^f \cos(\omega^f y + \psi_2^f) + \gamma_2^f \cos(\omega^f z + \rho_2^f)) \\ u_3^F(x, y, z) &= \sum_{f=1}^F (\alpha_3^f \cos(\omega^f x + \phi_3^f) + \beta_3^f \cos(\omega^f y + \psi_3^f) + \gamma_3^f \cos(\omega^f z + \rho_3^f)) \end{aligned} \quad (4)$$

where $X = (x, y, z)$ are the coordinates of the voxel in the reference image (i.e. the probability map extract from MR image) and $U^F(X) = (u_1^F(x, y, z), u_2^F(x, y, z), u_3^F(x, y, z))$ are the coordinates of the homologous points in the floating image (i.e. the normalized US image). The registration procedure can be written as :

$$\arg \max_{\mathbf{P}} \int_{\Omega} p(X \in \Phi_{MR}) \cdot p(U^F(X) \in \Phi_{US}) dX \quad (5)$$

where $\mathbf{P} : \{\alpha_i^f, \beta_i^f, \gamma_i^f, \phi_i^f, \psi_i^f, \rho_i^f; i \in [1, 2, 3]; f \in [1, \dots, F]\}$ represents the set of basis function parameters.

2.3. Optimization

These parameters are iteratively estimated from the lowest frequency to the highest frequency. First, the Simplex optimizer is used to estimate the 18 parameters for ω^1 . Then, these parameters are fixed and the 18 parameters for ω^2 are then estimated. This procedure is repeated until $f = F$. In the experiments, the same set \mathcal{W} was used for all the patients. This set is composed of 10 pulsations (i.e. $F = 10$) regularly distributed between $[\omega^1, \omega^{10}]$ such as $\omega^f = \frac{\pi}{2} \cdot f \cdot d$ with $d = 0.1$.

3. OVERALL WORKFLOW

The presented rigid and non-rigid registrations are integrated into a global workflow in order to (a) correct the error performed by the neuronavigation system and (b) compensate for the cerebral deformation occurring after opening the dura.

Preoperative stage : first, the T1-w MR image is denoised with a Non-Local (NL) means filter [14] in order to avoid false detections of hyperechogenic structures by the $MLvv$ operator (see left in Fig. 1). Then, the lesion is manually segmented by the neurosurgeon. Finally, the $MLvv$ is computed on the brain tissues. The probability maps from T1-w MR image is obtained by normalizing and fusing the positive values of the $MLvv$ with the lesion segmentation (see middle in Fig. 1). **Intraoperative stage :** *Before opening the dura* the first 3D freehand US sequence acquired on the dura was reconstructed [10] and denoised [11]. Then, the preoperative MR image was re-sliced into the US coordinate system thanks to the transformation matrix provided by the neuronavigation system (see top-left in Fig. 4 and Fig. 5). Finally, the rigid registration of the corresponding probability maps was performed in order to correct the error of the neuronavigation system (localization + initial rigid registration) and US probe calibration errors (see top-right in Fig. 5 and Fig. 4). *After opening the dura* the second freehand US sequence acquired on the cortical surface was reconstructed, denoised and projected into the coordinate system of the first US volume (see bottom-left in Fig. 4 and Fig. 5). By this way, the second US volume and the rigidly registered MR image can be overlaid in the same coordinate system. Then, the non rigid registration of the corresponding probability maps was performed in order to compensate for the brainshift (see bottom-right in Fig. 4 and Fig. 5).

3.1. Material

The preoperative T1-w MR image was acquired on a 3T Philips Gyroscan scanner. During the IGNS procedure, the US probe (Sonosite cranial 7 – 4MHz probe) was tracked by the Polaris cameras of the Stealth Station TREON (Medtronic Inc). The 3D freehand ultrasound sequences were acquired by the Sononav software installed on neuronavigator. The probe has been calibrated using a Z-wire phantom. The coordinate system of the preoperative MR image and the coordi-

nate system of the intraoperative field are related by a rigid registration performed by the neuronavigator at the beginning of the neurosurgical procedure. This rigid registration is based on surface matching between preoperative MR image and the position of points acquired on the patient’s head. All results presented in experiments on synthetic deformation and real data sets were obtained with the same parameters at each step of the workflow. At present, except the lesion segmentation during the preoperative stage, the processing workflow is fully-automatic. The computational times obtained on a Dual-Core Intel(R) Pentium(R) D CPU 3.40GHz for reconstructed US volumes with voxel size of (0.3,0.3,0.5) mm were : less than one minute for the reconstruction, around one minute for the US denoising and for the rigid registration, and less than 3 minutes for the non rigid registration.

4. EXPERIMENTS ON SYNTHETIC DEFORMATION

4.1. Evaluation framework

The quantitative evaluation of the proposed non rigid registration is based on simulated brain deformations. This simulation builds on properties of real brain deformations occurring during neurosurgery before lesion resection : the mean magnitude of the deformation (quantified around 3 and 4 mm in [3, 1]), the location of the maximal deformation (usually located under the craniotomy) and the cerebral falx stability. First, a neurosurgeon manually defined a realistic displacement for ten control points according to the mentioned properties of real brain deformations. The movement of the control points near the lesion under the craniotomy were chosen around 5.25 mm and the movement of the control points near the cerebral falx inferior to 1 mm. Then, the movement of the control points was extrapolated over all the volume thanks to thin plate spline functions (see Fig. 2). The parametrization of the extrapolation differs from the proposed parametrization in order to perform fair evaluation. Magnitude of the applied deformation is shown at bottom

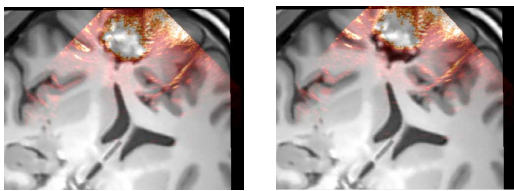


Fig. 2. Synthetic deformation. Left : Initial images used for the experiment. Right : Images warped with the simulated deformation.

left of figure 3. The magnitude was computed as the mean Euclidean distance between the original image and the deformed image over all voxels with intensities different to 0 and on the control points. The mean displacement over all the volume was 2.84 ± 1.11 mm with a maximal of 5.25 mm near the lesion. The mean displacement of the control points was 4.07 ± 1.17 mm with a maximum of 5.26 mm.

4.2. Quantitative results on synthetic deformation

The quantitative evaluation was performed by computing residual error after non rigid registration of the deformed US image and the preoperative MR image. The residual error was estimated as the mean Euclidean distance between the applied simulated deformation and the deformation estimated by the proposed non rigid registration procedure. After non rigid registration, the residual error over the volume decreased from 2.84 ± 1.11 mm up to 1.48 ± 0.56 mm. The residual error on the control points decreased from 4.07 ± 1.17 mm to 1.49 ± 0.66 mm. Figure 3 shows the result of the non rigid registration.

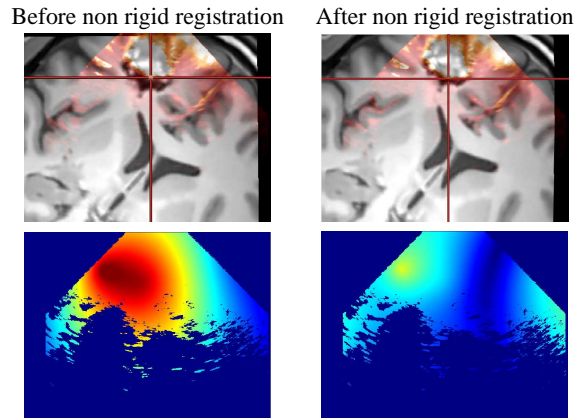


Fig. 3. Synthetic deformation. Top : Overlay of the denoised US and the resliced MR images before and after non rigid registration. Bottom : Distance norm between the US and MR images before and after non rigid registration.

5. RESULTS ON INTRAOPERATIVE DATA

The proposed approach was evaluated on 4 patient datasets. The accuracy of the registration was visually checked by the neurosurgeon over the volumes. According to the neurosurgeon, the overlay of the modalities was improved after rigid and non rigid registration procedures in all cases. Table

Table 1. Result of the overall workflow for 4 patients.

Patient	Rigid registration Estimated error	Non rigid registration Estimated deformation
1	5.72 mm	2.71 ± 1.03 mm
2	4.94 mm	3.74 ± 1.19 mm
3	6.50 mm	1.81 ± 1.02 mm
4	7.63 mm	0.09 ± 0.11 mm

1 shows the quantitative results obtained for the four patients after rigid and non rigid registration. These estimations were computed as the mean Euclidean distance over all the voxels before and after registration. The estimated errors produced by the neuronavigator were significantly higher than the errors reported in the literature (< 3 mm [6]). This difference

may be due to the clinical context of our study where the constraints differ from phantom studies. The magnitude of the estimated non rigid deformations was close to the deformation reported by others studies [3, 1, 2]. According to the neurosurgeon, in all cases, the rigid registration greatly improved the registration of the US and MR images performed by the neuronavigation system. Figures 4 and 5 show the result of the registration for patients 1 and 3.

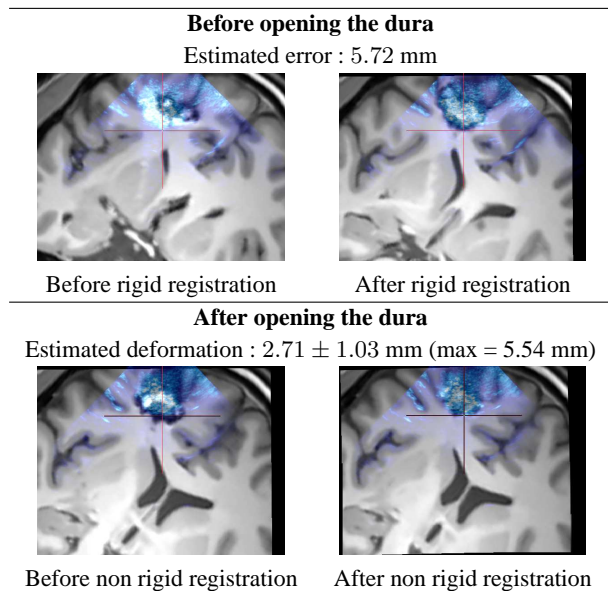


Fig. 4. Patient 1 with a cavernoma in prefrontal area. Top : result of the rigid registration before opening the dura. Bottom : result of the non-rigid registration after opening of the dura.

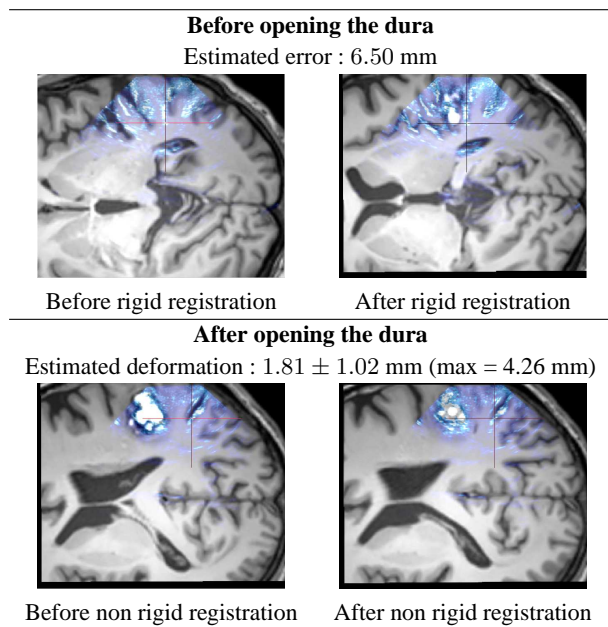


Fig. 5. Patient 3 with a cavernoma in central area. Top : result of the rigid registration before opening the dura. Bottom : result of the non-rigid registration after opening of the dura.

6. CONCLUSION

This paper presented a global framework designed for brainshift compensation. The proposed workflow is based on 3D freehand ultrasound imaging and 3D multimodal registration of US and MR maps at each step of the neurosurgical procedure. The multimodal registration is performed by matching the hyperechogenic structures of the brain. Quantitative evaluation with synthetic deformation was proposed to quantify the accuracy of the non rigid registration. The mean accuracy is estimated around 1.5 ± 0.5 mm over the registered volumes. Experiments on 4 patients with various pathologies show that our approach efficiently corrects the error performed by the neuronavigation system and fully-automatically compensates for the brainshift during intraoperative stage. The mean error of the neuronavigation system is estimated around 6.19 mm on the four studied cases. The mean deformations after opening the dura are estimated around 2.75 ± 1.08 mm when brainshift occurred. Further investigations need to be pursued on quantitative validation for the estimated deformations on real data sets. The proposed workflow takes around 2 minutes 30 seconds to correct the error of the neuronavigator system and around 4 minutes to compensate the brain deformations.

7. REFERENCES

- [1] C. Nimsky et al., "Quantification of visualization of, and compensation for brain shift using intraoperative magnetic resonance imaging," *Neurosurgery*, vol. 47, pp. 1070–1080, 2000.
- [2] A. Nabavi et al., "Serial intraoperative MR imaging of brain shift," *Neurosurgery*, vol. 48, no. 4, pp. 787–798, 2001.
- [3] M. M. J. Letteboer et al., "Brain shift estimation in image-guided neurosurgery using 3D ultrasound," *IEEE TBE*, vol. 52, no. 2, pp. 268–276, 2005.
- [4] A. Roche et al., "Rigid registration of 3D ultrasound with MR images : a new approach combining intensity and gradient information," *IEEE TMI*, vol. 20, no. 10, pp. 1038–1049, October 2001.
- [5] T. Arbel et al., "Automatic non-linear mri-ultrasound registration for the correction of intra-operative brain deformations," in *MICCAI*. 2001, vol. 2208 of *LNCS*, pp. 913–922, Springer.
- [6] R. M. Comeau et al., "Intraoperative ultrasound for guidance and tissue shift correction in image-guided neurosurgery," *Medical Physics*, vol. 27, pp. 787–800, 2000.
- [7] D. G. Gobbi et al., "Ultrasound/MRI Overlay with Image Warping for Neurosurgery," in *MICCAI*, 2000, vol. 1935 of *LNCS*, pp. 106–114.
- [8] I. Reinertsen et al., "Validation of vessel-based registration for correction of brain-shift," *MedIA*, vol. 11, no. 4, pp. 374–388, June 2007.
- [9] P. Coupé et al., "A probabilistic objective function for 3D rigid registration of intraoperative US and preoperative MR brain images," in *IEEE ISBI*, 2007, pp. 1320–1323.
- [10] P. Coupé et al., "Probe Trajectory Interpolation for 3D Reconstruction of Freehand Ultrasound," *MedIA*, vol. 11, no. 6, pp. 604–615, 2007.
- [11] P. Coupé et al., "Nonlocal means-based speckle filtering for ultrasound images," *IEEE TIP*, vol. 18, no. 10, pp. 2221–2229, 2009.
- [12] J.B.A Maintz et al., "Evaluation of ridge seeking operators for multi-modality medical image matching," *IEEE PAMI*, vol. 18, pp. 353–365, 1996.
- [13] J. Ashburner and K. J. Friston, "Nonlinear spatial normalization using basis functions," *HBM*, vol. 7, no. 4, pp. 254–266, 1999.
- [14] P. Coupé et al., "An Optimized Blockwise NonLocal Means Denoising Filter for 3-D Magnetic Resonance Images," *IEEE TMI*, vol. 27, no. 4, pp. 425–441, April 2008.